Characterization of Operational Performance of Ka-band Links in Deep Space Network

Timothy Pham, Jason Liao
Jet Propulsion Laboratory
California Institute of Technology
Pasadena, California, USA
E-mails: Timothy.Pham@jpl.nasa.gov Jason.Liao@jpl.nasa.gov

Abstract - This paper presents a characterization of performance of 32-GHz Ka-band link in an operational environment. The data come from tracking of Kepler spacecraft by the NASA Deep Space Network (DSN) in the past few years. Ka-band link offers a significant signal-to-noise advantage compared to the more common X- or S-band; however, it is subject to more signal fluctuation caused by the weather. Kepler is the first mission supported by the DSN that solely rely on the higher deep space Ka-band communications link to return its high-rate science data. A well characterization of the operational performance of Kepler would benefit future Ka-band missions, especially for those operating with smaller link margin.

The study examines how weather conditions at the DSN facilities (e.g., winds, clouds, rains) affect the received signal, particularly on telemetry data. It addresses questions such as how often the weather affects the link and how much degradation the link could suffer. Among the 22 Ka-band passes in 2012, heavy clouds affected one pass and two passes were impacted by high winds. The adverse weather caused at time as much as 3-dB instantaneous change in the signal to noise ratio (SNR). Estimates of degradation to the SNR as a function of wind speeds are captured based on observations.

This study also quantifies the probability distribution of the variation of received signal power. With such information, future missions can better plan their link design. An optimal link design aims for just having enough margin to realize the data return with a targeted probability, with neither having too much margin that it reduces the downlink data rate nor insufficient reserve that causes frequent data outages. The study tries to provide some answers to the questions such as how much does SNR vary from one tracking pass to the next, and what is the cumulative distribution of signal fluctuation. Regarding the signal variation over many tracking passes, we found that the averaged symbol SNR (SSNR) for each pass changed by as much as 4 dB. Some variations were due to geometry such as the changing distance between spacecraft and Earth and different antenna pointing elevations. Other variations seem to be random in nature, reflecting the randomness of operational environments. Some passes were found to be quite stable, with a standard deviation of symbol SNR around 0.25 dB while others had greater variation, up to 1.4 dB. Overall, the cumulative distribution of the symbol SNR reflects that 50% of the fluctuations was less than 0.6 dB, 90% of fluctuation was within 1.6 dB and 95% within 2.2 dB.

Some of the challenges in data processing, validation and modeling were captured in this paper. We observed some inconsistent measurements where operational data significantly deviate from a normal expectation. These inconsistent measurements made it hard to develop an accurate and consistent performance model, such as the degradation of signal SNR as a function of high wind. The difficulty was compounded by the fact that there were only a few Ka-band passes observed in high winds.

I. INTRODUCTION

The National Aeronautics and Space Administration (NASA) Deep Space Network (DSN) serves as a communications infrastructure to enable mission controllers communicate with their spacecraft exploring the outer space. The DSN currently comprises of 13 antennas operating at multi-frequency of 2 GHz S-band, 8 GHz X-band and 26 GHz & 32 GHz Ka-band. The majority of 30-plus missions supported by the DSN use X-band. A few still use the narrower S-band while some are moving to the new broader Ka-band. Compared to X-band operation, Ka-band offers missions greater bandwidth that better supports higher data rates. The International Telecommunications Union allocates about 500 MHz for deep space Ka-band (32 GHz) and 1.5 GHz for the near Earth Ka-band (26 GHz), compared to 45 MHz each for deep space and near Earth X-band. Ka-band operation also offers roughly 5.5 dB advantage in the signal-to-noise ratio (SNR) performance, compared to the X-band operation, assuming the same transmitting power [1]. The 5.5 dB advantage is a result of a higher antenna gain at Ka-band due to greater operating frequency, mitigated by the higher system noise temperature.

Kepler mission is the first deep space mission that uses the 32-GHz deep space Ka-band as an operational link for telemetry return. The higher link performance, afforded by a higher SNR compared to the X-band link, allows for faster data downlink and enables spacecraft to devote more time on the collection of science data. Although Ka-band downlink was conducted on some earlier missions, such as the Mars Global Surveillance (MGS) and Mars Reconnaissance Orbiter (MRO), it was only for the purpose of technology demonstration - X-band was and still is the primary link for telemetry return. Two ongoing missions - Cassini and Juno – have a Ka-band signal, but it is a carrier-only (without modulated telemetry), mainly for radio science investigations. The received carrier's power, frequency and phase are used to infer the characteristics of planetary medium traversed by the signal.

Kepler mission has the advantage of operating at high SNR. Its healthy designed link margin, in the range of 4-5 dB, provides greater buffer to the impact of inclement weather. Other Ka-band missions to be launched in the near future, such as the Solar Probe Plus, will be operating with a smaller link margin. Thus, there is a strong interest in characterizing the link performance and signal fluctuation to enable better link design for future missions.

In this paper, we examine the data collected from Ka-band tracking of Kepler over a yearlong period and try to provide the answer to these questions:

(1) What is the typical variation in the signal SNR from one tracking pass to the next?
(2) How often does rain or clouds negatively affect the link and cause data outage? How much is the link affected by rains or heavy clouds?
(3) How often do high winds affect the antenna pointing accuracy and thus the link performance? How much degradation does the signal experience?
(4) What is the cumulative probability distribution of the signal fluctuation?

In Section II, we briefly describe the Ka-band operations of Kepler mission. General observations of the received signal characteristics, especially their variation from pass to pass, are discussed in Section III. Passes affected by the rains, clouds and high winds are discussed in Section IV and Section V, respectively. Section VI examines the statistics of signal power fluctuations. Conclusions are captured in Section VII.

II. KA-BAND OPERATIONS

The DSN has three tracking complexes spread evenly across the Earth longitudes in order to maintain a constant visibility with spacecraft in deep space. The three complexes are named the Goldstone, Canberra and Madrid Deep Space Communications Complexes, based on its location in the United States, Australia and Spain. The majority of the antennas are 34-m, with one 70-m at each site. Goldstone Complex currently has five operating antennas devoted to spacecraft tracking. Madrid and Canberra Complex each has four antennas. Within each complex, two 34-m antennas are equipped with 32-GHz Ka-band reception that can be used to support Kepler and other missions, such as Cassini and Juno. For a complete description, the DSN also supports the 26-GHz near-Earth Ka-band with one 34-m antenna at each complex. The near-Earth Ka-band is relevant to some near future missions, such as the Transiting Exoplanet Survey Satellite (TESS) in 2017 and the James Webb Space Telescope (JWST) in 2018. The analysis of this paper is done with the 32 GHz Kepler data; however, the findings should be applicable to the operations at 26-GHz near-Earth Ka-band due to spectral proximity.

The Kepler spacecraft uses two different frequencies, X- and Ka-band, for return telemetry data. The spacecraft relies on X-band for the return of low-rate spacecraft engineering data (up to 16 kbps) and for radiometric measurement (e.g., Doppler and ranging). X-band tracking occurs every three or four days, more often than Ka-band tracking. Once a month, when the science data buffer onboard spacecraft is nearly full, Kepler spacecraft would turn its Ka-band high gain antenna to Earth and downlink the high-rate science data (up to 4.3 Mbps) that are collected over the month-long observations. The Ka-band downlink sessions last several hours and typically take place over two DSN complexes. X-band data are also received concurrently with Ka-band. The dual-frequency links offer an opportunity to validate the observed signal fluctuation. If it is caused by common source of errors, such as bad weather or pointing problem on the ground or flight antenna, the effect would show up in both links, with a smaller effect expected on the lower X-band frequency link.

III. SIGNAL VARIATIONS

In this section, we look at the performance characteristics of Kepler Ka-band passes. Fig. 1 shows the link characteristics of all Ka-band passes in 2012. For each pass, the average telemetry symbol SNR (SSNR) and associated standard deviation, the observed SSNR minima and maxima are plotted. The label "DOYxx/DSS-xx" indicates the day of year (DOY) the pass took place and the antenna – Deep Space Station (DSS) – used for tracking (Goldstone: DSS-25 and -26; Canberra: DSS-34 and -35; Madrid: DSS-54 and -55).

The data reflect the following observations:

1. The average SSNR varied quite significantly among the passes, as much as 4.8 dB (2.3 dB - 7.1 dB). Some factors affecting the variation are:
(a) There is some performance difference among the DSN antennas used for the tracks.
(b) Tracking passes are done at different elevation, as dictated by the selected antenna and the time of actual downlink within the pass. This results in different system noise temperature level.
(c) Different data rates are used in the downlink, which affects the signal energy and thus, the symbol SNR.
(d) Change in the spacecraft range from Earth.
(e) Potential degradation from the rains/clouds or winds.

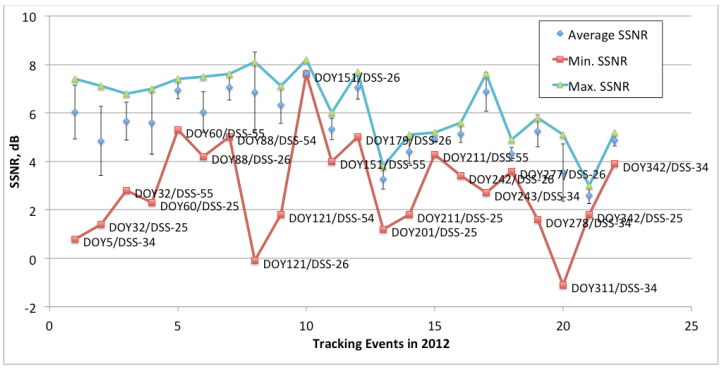

Fig. 1. SNR characteristic of Kepler Ka-band passes

One could theoretically normalize these geometric and link variations among the data of different passes to remove the effect of factors (b), (c) and (d). That would have resulted in a smaller variation, leaving just the effect of factors (a) and (e) remained. As a note, we estimate that the variation due to the ground and spacecraft antenna pointing error was small (less than 0.2 dB) because of the active conical scanning tracking used in the ground antenna pointing and because of spacecraft pointing precision driven by stringent science objectives.
On the link robustness, we note that the average SSNR of all Ka-band passes is about 5.5 dB. That level provides a healthy 6.2 dB link margin relative to the -0.7 dB threshold required for successful decoding of the concatenated convolutional (7, ½) and Reed Solomon (255, 232) codes that is employed in Kepler link. With such a large margin, it is expected that Kepler link be well protected against potential outages.

2. The standard deviations also varied among the passes. Some passes had standard deviation as small as 0.25 dB while others had deviation up to 1.4 dB. The passes with small standard deviation demonstrate that the SSNR measurements are stable down to 0.25 dB level. The passes with large standard deviation prompt a greater interest because they reflect atypical conditions that can negatively affect the link design. Two of these passes - DOY121/DSS-26 & DOY243/DSS-34 – were exposed to high wind, up to 45 kph. One pass - DOY32/DSS-55 - experienced rain. Other passes, such as DOY211/DSS-25, had a large SSNR fluctuation but the cause was not well understood. More specific detailed analysis of these atypical passes is discussed later in Section VI.

3. The SSNR minima generally lie further away from the average SSNR. Some of them were in the 3-sigma range, such as the passes on DOY121, DOY247 and DOY311. This large difference indicates that the signal likely experienced some large SNR drops caused by short bursts of impact.

4. The SSNR maxima generally lie close to the average values, not too far from the upper 1-sigma point. This is due to a non-Gaussian distribution of the measurements, as later seen in Section VI, where most of the points are close to the maximum SNR level. They are not separated from the average values by 2 - 3 sigma.

There are a few observations about the data processing:

(1) Kepler occasionally changes the data rate in mid pass. So, the computation of representative metrics for the link performance – SSNR average, standard deviation, minima and maxima - need proper filtering to single data rate. Without such filter, the computed link metrics, especially the standard deviation, would be larger than what they actually are.

(2) Data on Ka-band link need to be separated from the X-band link. However, the positive benefit of having concurrent X-band data is that we can use it to validate the common impacts caused by environmental factors, such as winds and rains.

(3) Some of the passes were configured with dual receivers on Ka-band, for redundant processing. We expect that the measurements from both receivers would be within the 0.25 dB measurement noise indicated earlier. Such consistency can be seen in the upper plot of Fig. 2 for DOY032/DSS-55 pass, where the difference between the two receivers was within 0.1 dB. Yet, there are passes where we observed a greater difference, as shown in the lower plot of Fig. 2 for DOY342/DSS-25 pass. Here, the SSNR measurements reported by the two receivers differed on the average by 0.7 dB.

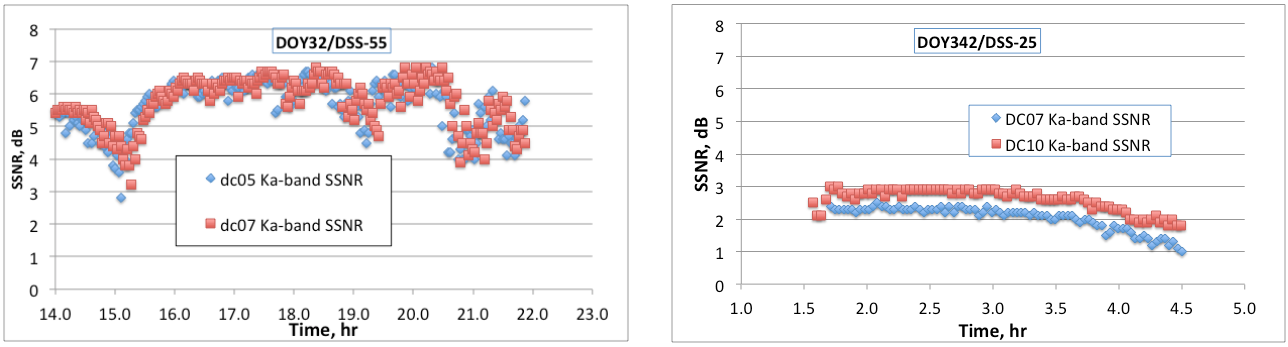

Fig. 2. Variation of SSNR measurements from the two receivers on the same antenna in DOY32/DSS-55 and DOY342/DSS-25 passes

Fortunately, in this study, since we are less concerned with the absolute SSNR level between passes and more interested in the signal fluctuation within the pass, this measurement difference does not negatively affect the analysis. If our analysis objective were to evaluate the loss in the ground system, this difference would have some impact.

Note that Kepler spacecraft experienced a failure with its second gyroscope in May 2013. This has affected the spacecraft ability to maintain a really stable platform for science observation. In 2015, after the flight team found a solution to improve the stability of spacecraft platform, the mission resumed its science observation; however, with a less stable platform, we observed a greater SSNR variation during the pass. A sample of a recent tracking pass, 2015 DOY114/DSS-34, is shown in Fig. 3. Given the pronounced periodic variations up to several dB, we feel that the data post the gyroscope failure are not useful to the analysis of pass-to-pass SSNR variation, compared to the data prior to mid 2013.

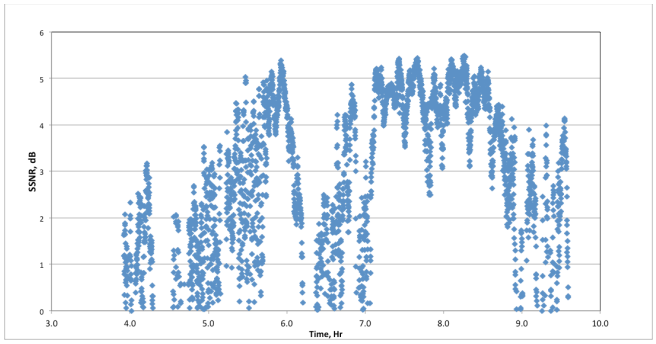

Fig. 3. Variation of symbol SNR on 2015, DOY114/DSS-34

IV. Impact of Rains/Clouds

In 2012, there was one Ka-band passes affected by rain or heavy clouds. The water content in the air column reduced the SSNR by as much as 3 dB. Fig. 4 shows the SSNR variations in DOY32/DSS-55 pass over Madrid. The Ka-band SSNR measured by both receivers reflected a 3 dB, 2.5 dB and 3 dB drop near the time15:00 hr, 19:00 hr and 21:00 hr, respectively. The X-band SSNR showed a similar degradation but with smaller impact, in the order of 1 dB, as expected. The drops in SSNR matched with the increases in the system noise temperature (SNT) around the same time. This correlation implies an impact from the external environment.

Each DSN Complex has a weather station that measures the wind speed/direction, humidity and precipitation. The precipitation data reflects the rainfall as measured by a rain gauge. The weather station however does not provide measurement on cloudiness where the water content in the air column would affect the system noise temperature and causing signal degradation. For the DOY32/DSS-55 data set, despite the presence of the SSNR variation, there was no indication of rainfall from the precipitation measurement. The absence of rain would make it hard to pinpoint the link between the SSNR degradation and weather. The only available collaborating evidence is the increase in the measured system noise temperature. Fortunately, we are able to independently confirm the system noise temperature measurement with the data from special research equipment called the Advanced Water Vapor Radiometer (AWVR) that independently measures the water content in the air. The AWVR is available at Goldstone and Madrid complex, but not Canberra, and has been in operations for over two decades. The AWVR measures the sky brightness temperature at 31.4 GHz [2]. The water vapor radiometer data are collected continuously throughout the day, one sample every 10 minutes. The measurements are done at zenith but the data can be translated to any elevation of interest so that they can be compared with the measured system noise temperature of the pass (which is done by a different set of equipment, using the Y-factor method with a small injected noise-diode) [3]. This AWVR elevation translation however produces a uniform estimated noise temperature in all azimuth directions. In contrast, the SNT measurement is azimuth specific because the measurement is done along the line of sight of antenna tracking spacecraft. So, there may be some difference in the absolute measurements between the two data sets. Nevertheless, we found the data with reasonable consistency. Fig. 5 shows the AWVR-derived noise temperature on DOY32 at 40-deg elevation, approximately the same elevation of Kepler tracking at 21:00 hr. [4].

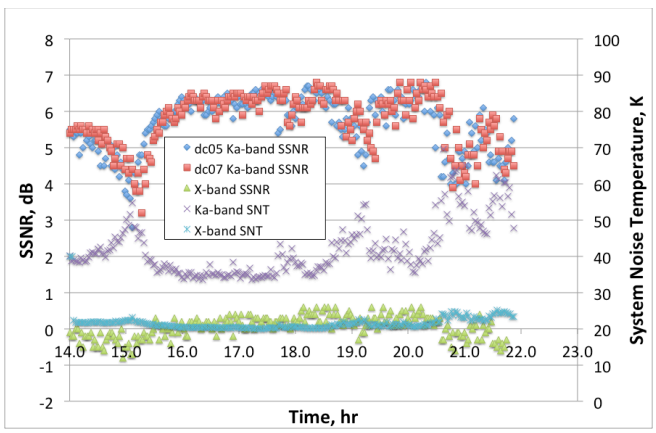

Fig. 4. Variation of symbol SNR and system noise temperature at Ka- and X-band on DOY32/DSS-55

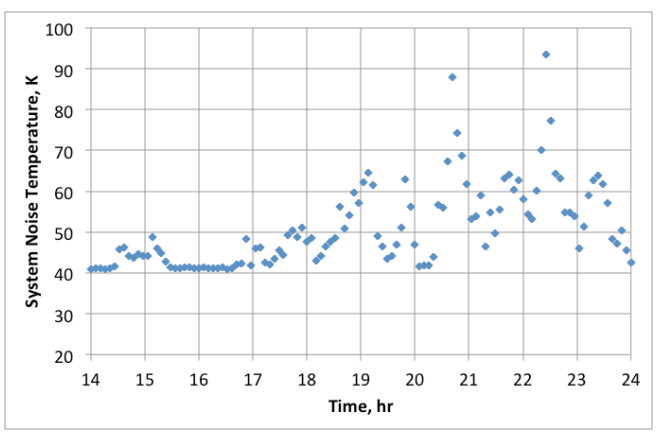

Fig. 5. AWVR system noise temperature for DOY32/DSS-55

The temperature is observed to vary significantly at 18:00 hr, with big bursts of 30 K or more near 21:00 hr, which is consistent with the variation seen in the SNT measurement in Fig. 4.

V. Impact of Winds

In this section, we look at a few sample passes with relative high winds, above 40 kph. In one particular pass on 2015, DOY114, the wind even reached to 70 kph, not a common occurrence. From these samples we would draw some estimates on the SNR degradation caused by the winds.

However, the collected data are not always consistent and some judgments are necessary to exclude invalid data so that they would not distort the analysis. In the following discussion, we examine two tracking passes - DOY121/DSS-26 at Goldstone and DOY243/DSS-34 at Canberra, both with high wind condition, up to 45 km/hr. The impact of wind on the SNR degradation was quite apparent on DOY243 while it was more ambiguous on DOY121.
Fig. 6 shows the measurements of symbol SNR and carrier SNR (Pc/No), as well as the system noise temperature and wind speed on DOY243. Both the SSNR and Pc/No showed high level of fluctuation during the first hour of the pass. Several big drops in SNR occurred at the same time for both measurements, indicating the phenomenon was real rather than just a measurement error. The relatively constant system noise temperature implied that the variation in the SNR was in the signal power reduction rather than in the increased noise (as caused by rains or clouds). There were high winds, up to 45 kph, in the earlier part of the track. Some of the highest peaks of wind speed aligned with the drops in the SSNR and Pc/No, as much as 4 dB. These sudden SNR drops are what cause the SNR minima of the pass to be much lower than the one-sigma point below the average SSNR, as mentioned earlier in Section III.

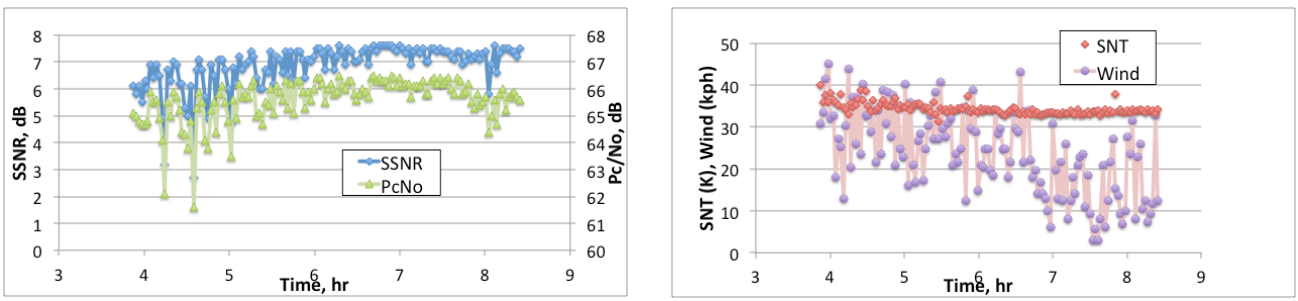

Fig. 6. Variation of SSNR, system noise temperature and wind speed on DOY243/DSS-34

There seems to be less consistency among the collected measurements in the DOY121/DSS-26 data set. Fig. 7 plots the SSNR, Pc/No, system noise temperature and wind speed for that pass. Both SSNR and Pc/No showed a drop around the time of 23.8 hr., but with different characteristics. While the SSNR drop was prominent and abrupt - as much as an 8 dB in less than 6 minutes - the Pc/No drop was more gradual, just about 1 dB over 20 minutes. The observed wind speed at this point was about 40 kph, which seemed to be not strong enough to cause either a drop of lock or an 8-dB degradation (compared to the DOY243 data). This raised an uncertainty on the SSNR measurement over this period of impact. Although the symbol tracking was reported to be in lock, we suspect it might be in error and the possible drop of lock could have affected the validity of the reported SSNR.

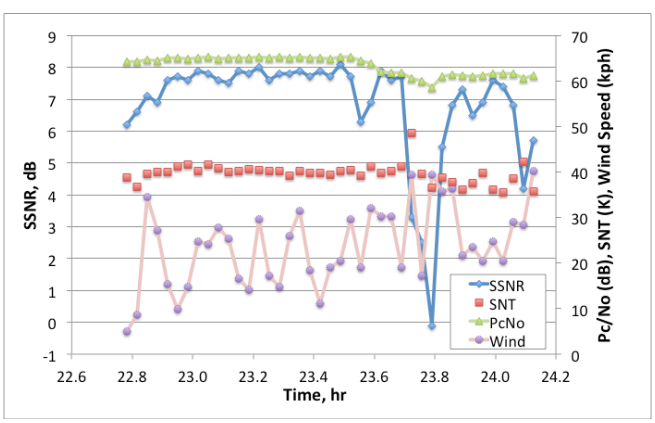

Fig. 7. Variation of SSNR, system noise temperature and wind speed on DOY121/DSS-26

We examined the effect of the winds by looking at the correlation between the SSNRs and the wind speeds. However, it should be noted that the varying system noise temperatures for different antenna pointing elevations within a pass

would affect the SSNR measurements. Low antenna elevation yielded a higher system noise temperature and lower SSNR than those at higher elevation, because of a more extended path length that the signal traversed through the Earth atmosphere. The spatial cloud distribution on a cloudy day, as discussed in Section IV, could also cause a variation in the system noise temperature and subsequently SSNR. In addition, the SSNR could also be changed if there is a change in the downlink data rate. These effects needed to be accounted for before we could properly analyze the impact of winds on the SSNR.

Fig. 8 shows the SSNR as a function of wind speed for six different passes with high winds that we analyzed. In general, one could see a negative effect of high winds on the signal SSNR, i.e., the SSNRs getting smaller and the measurements more scattered. Yet, the data were not always consistent. Some passes (e.g., 2012 DOY121, 2012 DOY 243 and 2015 DOY114) showed a strong correlation while others, such as 2013 DOY125, showed a much smaller causal effect.

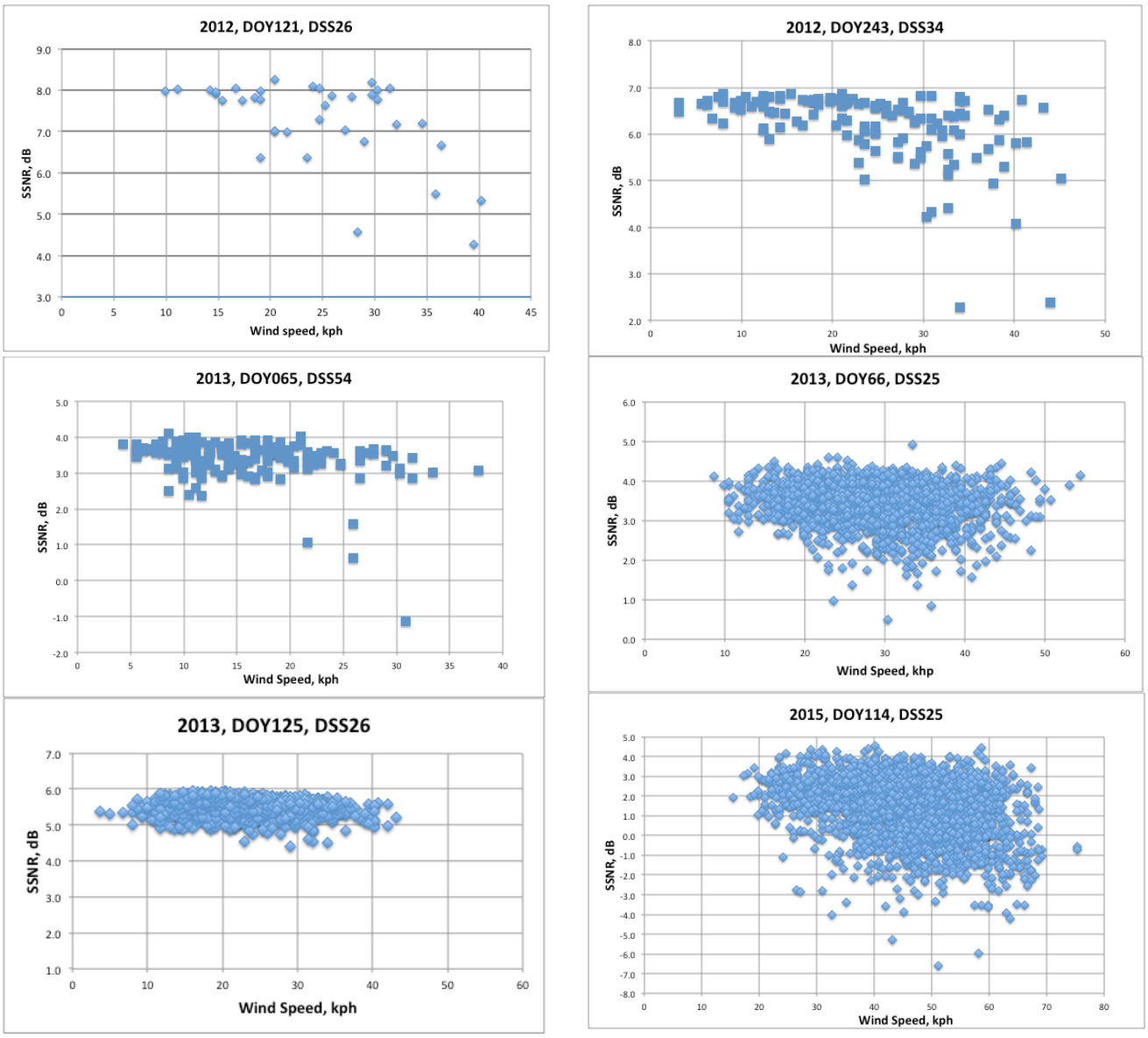

Fig. 8. Correlation of signal SSNR and wind speed on four different passes with significantly high winds

Each data set in Fig. 8 are least-squared fit with a second order polynomial, which is then used to compute the SSNR degradation. Table 1 approximates the degradation at various wind speeds between 20 kph and 70 kph, relative to that at the 10-kph winds where the loss is considered to be minimal. The SSNR scattering at various wind conditions are

presented in Table 2. Larger SSNR scattering at higher winds implies a potential signal instability that could affect the success of data downlink. Missions that want to return a high percentage of data under high wind conditions would have to reserve sufficient margin to accommodate the lowest observed SSNRs, rather than just the averaged degradation shown in Table 1.

Table 1. Averaged degradation in SSNR at different wind speeds, relative to 10 kph winds

	Additional degradation relative to 10 kph wind, dB										
Kepler Tracking Passes	20 kph	25kph	30 kph	35 kph	40 kph	45 kph	50 kph	55 kph	60 kph	65 kph	70 kph
2012, DOY243, DSS34	-0.3	-0.4	-0.7	-0.9	-1.3	-1.6	-2.1				
2013, DOY65, DSS54	-0.3	-0.4	-0.6	-0.8	-1.1						
2013, DOY66, DSS25	-0.1	-0.2	-0.2	-0.3	-0.3	-0.3	-0.2				
2013, DOY125, DSS26	0.0	0.0	0.0	-0.1	-0.2	-0.2					
2015, DOY114, DSS25	-0.1	-0.2	-0.3	-0.5	-0.6	-0.8	-1.1	-1.3	-1.6	-1.9	-2.3

Table 2. Variation of SSNR measurements at various wind speed

Kepler Tracking Passes	Scattering of SSNR, dB					
	20 kph	30 kph	40 kph	50 kph	60 kph	70 kph
2012, DOY243, DSS34	0.8	1.6	2.8			
2013, DOY65, DSS54	1.2	insufficient data	insufficient data			
2013, DOY66, DSS25	2.0	2.4	2.8			
2013, DOY125, DSS26	1.2	1.4	0.7			
2015, DOY114, DSS25	3.0	4.0	5.0	6.0	7.0	insufficient data

The above example reflects some of the challenges with data processing, e.g., what to include vs. exclude in the data analysis in order to arrive at the right model. Some operational measurements are not as consistent as we like.

VI. SIGNAL FLUCTUATION STATISTICS

We are interested in characterizing the probability distribution of the signal variations to aid with the link design in future missions. In an ideal case, if there were accurate prediction on the signal SNR, any operational degradation would be reflected as a deviation of the measurement from the prediction since the prediction are model-based and have no knowledge of real-time weather impact. Unfortunately, predictions are not available with Kepler Ka-band passes.

To compensate for the lack of SNR prediction, we calculate the fluctuation by a degradation against the maximum SSNR of the pass, as discussed in Section V. Additional adjustment is also needed since both the antenna gain and system noise temperature change as a function of antenna elevation [5]. The antenna gain is affected by the gravity distortion of the antenna structure. The system noise temperature varies due to different path length through the Earth atmosphere that the signal traverses at different elevation. Lower elevation results in a higher noise temperature because of the longer atmospheric path.

For each pass, the measured SSNR's are subtracted from the SSNR maxima of the pass. Fluctuation data of all Ka-band passes in 2012 are then combined to generate the cumulative distribution function of SNR variation, as shown in Fig. 10. The distribution shows that 50% of the fluctuations are less than 0.6 dB, 90% are within 1.6 dB, and 95% being less than 2.2 dB.

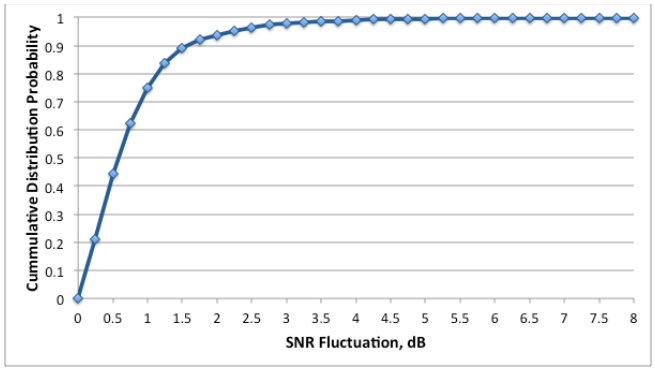

Fig. 10. Cumulative distribution of SNR fluctuation

VII. CONCLUSION

In summary, this paper examined the variation of Kepler Ka-band signal observed from the DSN tracking. In benign conditions, the SSNR measurements within a pass were stable within 0.25 dB. In adverse weather of heavy clouds or winds, the SSNR within the pass varied as much as 1.5 dB (1-sigma). Out of 22 Ka-band passes in 2012, one pass was affected by the heavy clouds (no rain) and two passes impacted by high winds. These effects could cause an instantaneous change of SNR by up to 3 dB. Kepler mission, however, has a robust link with an average 6.2 dB margin, which helps minimizing the telemetry data outage. The cumulative distribution of the SSNR variation shows that 50% of the variation are within 0.6 dB of the maximum SSNR within the tracking pass, 90% are within 1.6 dB and 95% within 2.2 dB.

Through this analysis, we learned that one has to be careful with the data selection. Since a track could involve multiple receivers at multiple frequency (X- and Ka-band) and multiple data rates (spacecraft can change data rate within the pass to preserve link margin), proper filtering of data is essential for valid data compilation and analysis. Compensation for the changing elevations in the signal SNR is required to normalize the data to the same conditions. We also learned that while measurements from two different receivers of the same received Ka-band signal are generally the same to within 0.25 dB, at times they could differ by as much as 0.75 dB. This difference would have a greater impact on future studies, such as characterization of system loss that are dependent on the absolute, rather than relative, accuracy of the SSNR measurements.

In the future, we plan to extend the analysis of link performance beyond the SSNR realm and into the telemetry frame error statistics. Those statistics should give us more insights on how the Ka-band link performs on the fast time scale of milliseconds where the telemetry frames reside.

ACKNOWLEDGMENT

The work described in this paper was carried out by the Jet Propulsion Laboratory, California Institute of Technology, under a contract with the National Aeronautics and Space Administration.

REFERENCES

[1] S. Shambayati, "A Comparison of the Ka-band Deep-Space Link with the X-band Link Through Emulation," The Interplanetary Network Progress Report 42-178, Jet Propulsion Laboratory, Pasadena, California, August 15, 2009, p. 48.

[2] A. Tanner and A. Riley, "Design and Performance of a High Stability Water Vapor Radiometer," Radio Science, vol. 38, no. 3, March 2003, pp.15.1–15.12.

[3] C. T. Stelzried, R. C. Clauss, and S. M. Petty, "Deep Space Network Receiving Systems' Operating Noise Temperature Measurements," The Interplanetary Network Progress Report 42-154, April–June 2003, Jet Propulsion Laboratory, Pasadena, California, August 15, 2003, pp. 1–7.

[4] S. Slobin, personal communications, Jet Propulsion Laboratory, Pasadena, California, October 15, 2015.

[5] DSN Telecommunications Link Design Handbook (810-005), Module 104, 34-m BWG Antennas Telecommunications Interfaces, Jet Propulsion Laboratory, Pasadena, California, April 1, 2015, pp. A-1–A-12.